www.impactjournals.com/oncotarget/ Oncotarget, 2018, Vol. 9, (No. 17), pp: 13834-13847

Research Paper

Bcl-xL as a poor prognostic biomarker and predictor of response to adjuvant chemotherapy specifically in *BRAF*-mutant stage II and III colon cancer

Philip D. Dunne[1,*], Helen G. Coleman[1,2,*], Peter Bankhead[1], Matthew Alderdice[1], Ronan T. Gray[2], Stephen McQuaid[1], Victoria Bingham[1], Maurice B. Loughrey[2], Jacqueline A. James[1], Amy M.B. McCorry[1], Alan Gilmore[1], Caitriona Holohan[1], Dirk Klingbiel[3,7], Sabine Tejpar[4], Patrick G. Johnston[1], Darragh G. McArt[1], Federica Di Nicolantonio[5,6], Daniel B. Longley[1] and Mark Lawler[1]

[1]Centre for Cancer Research and Cell Biology, Queens's University Belfast, Belfast, UK

[2]Centre for Public Health, Queens's University Belfast, Belfast, UK

[3]SAKK Swiss Group for Clinical Cancer Research, Coordinating Center, Bern, Switzerland

[4]Digestive Oncology Unit, University Hospital Gasthuisberg, Leuven, Belgium

[5]University of Turin, Department of Oncology, Candiolo, Turin, Italy

[6]Candiolo Cancer Institute - FPO, IRCCS, Candiolo, Turin, Italy

[7]SIB Swiss Institute of Bioinformatics, Bioinformatics Core Facility, University of Lausanne, Lausanne, Switzerland

[*]Joint first authors

Correspondence to: *Philip D. Dunne,* ***email:*** *p.dunne@qub.ac.uk*
Mark Lawler, ***email:*** *mark.lawler@qub.ac.uk*

Keywords: *colon cancer; gene expression profiling; molecular stratification; relapse risk; Bcl-xL*

Received: *January 30, 2018* ***Accepted:*** *February 05, 2018* ***Published:*** *February 13, 2018*

ABSTRACT

Purpose: BRAF mutation occurs in 8–15% of colon cancers (CC), and is associated with poor prognosis in metastatic disease. Compared to wild-type BRAF (BRAFWT) disease, stage II/III CC patients with BRAF mutant (BRAFMT) tumors have shorter overall survival after relapse; however, time-to-relapse is not significantly different. The aim of this investigation was to identify, and validate, novel predictors of relapse of stage II/III BRAFMT CC.

Experimental design: We used gene expression data from a cohort of 460 patients (GSE39582) to perform a supervised classification analysis based on risk-of-relapse within BRAFMT stage II/III CC, to identify transcriptomic biomarkers associated with prognosis within this genotype. These findings were validated using immunohistochemistry in an independent population-based cohort of Stage II/III CC (*n* = 691), applying Cox proportional hazards analysis to determine associations with survival.

Results: High gene expression levels of Bcl-xL, a key regulator of apoptosis, were associated with increased risk of relapse, specifically in BRAFMT tumors (HR = 8.3, 95% CI 1.7–41.7), but not KRASMT/BRAFWT or KRASWT/BRAFWT tumors. High Bcl-xL protein expression in BRAFMT, untreated, stage II/III CC was confirmed to be associated with an increased risk of death in an independent cohort (HR = 12.13, 95% CI 2.49–59.13). Additionally, BRAFMT tumors with high levels of Bcl-xL protein expression appeared to benefit from adjuvant chemotherapy (P for interaction = 0.006), indicating the potential predictive value of Bcl-xL expression in this setting.

Conclusions: These findings provide evidence that Bcl-xL gene and/or protein expression identifies a poor prognostic subgroup of BRAFMT stage II/III CC patients, who may benefit from adjuvant chemotherapy.

INTRODUCTION

Signaling through the Epidermal Growth Factor Receptor (EGFR) pathway is a common event in cancer development [1], with activating mutations in *KRAS, NRAS* and *BRAF* occurring in approximately 50% of colorectal cancer (CRC) patients [2]. Results from a phase III trial (MRC COIN trial, $n = 1630$) in metastatic CRC revealed that patients with *BRAF* mutant (*BRAFMT)* tumors have a significantly worse prognosis compared to patients with *KRAS* mutant (*KRASMT)* tumors or tumors with no detectable mutations in *KRAS* or *BRAF* (*WT/WT*) [3]. The use of a *BRAFMT* specific inhibitor, vemurafenib, in advanced melanoma, has improved survival rates for patients with this activating mutation [4], and underpinned the rationale for a phase Ib study employing vemurafenib in *BRAFMT* CRC [5]. Unfortunately, unlike the encouraging results observed in *BRAFMT* melanoma, the inhibitor did not benefit *BRAFMT* CRC patients in the advanced disease setting. Mechanistic studies have indicated that resistance to vemurafenib in CRC is due to feedback activation of the EGFR pathway [6], further highlighting the key role played by EGFR signaling in CRC.

To examine the role of *BRAF* in the adjuvant stage II/III disease setting, Popovici and colleagues performed differential gene expression analysis to identify transcriptional differences between *BRAFMT* and *BRAFWT/KRASWT* tumors in a cohort of 688 stage II and III colon cancer (CC) clinical trial samples (PETACC-3) [7]. Their analysis identified the distinct underlying biology of the *BRAFMT* subgroup. Furthermore, the authors generated a 64-gene classifier, which stratified the cohort into two subgroups. The first subgroup, which accounted for 27% of the cohort, displayed a transcriptional signature similar to *BRAFMT* tumors (termed "pred-BRAFm") and had a worse prognosis in terms of overall survival (OS) and survival-after-relapse compared to the second subgroup, which had a signature similar to that of *BRAFWT* disease (termed "pred-BRAFwt"). Critically however, while both *BRAF* mutation and the pred-BRAFm signatures could identify subgroups of patients with poorer OS *after* relapse (i.e. when the patient had progressed to stage IV metastatic disease), the rates of disease relapse in these subgroups were not significantly different to *BRAFWT* and pred-BRAFwt disease.

There is currently a lack of understanding of the biology that drives disease relapse specifically within stage II/III *BRAFMT* disease, resolution of which could ultimately inform treatment of a clinically-definable subgroup of *BRAFMT* patients, who have the worst prognosis when they progress to stage IV, but who still may be potentially curable in stage II/III. Therefore, we aimed to identify novel predictors of relapse for stage II/III *BRAFMT* CC, employing transcriptomic datasets for *in silico* discovery/initial corroboration, followed by subsequent validation of promising lead candidate(s) from bioinformatics analyses by immunohistochemistry analysis within a large population-based stage II/III *BRAFMT* CC study.

RESULTS

Study outline and rationale for risk stratification in BRAFMT CC

We analyzed available transcriptional data from the well-characterized dataset, GSE39582, as outlined in Supplementary Figure 1. Compared to *KRASMT* and *WT/WT* patients, *BRAFMT* patients were significantly more likely to be older ($p < 0.001$), have proximal tumors ($p < 0.001$) that exhibited microsatellite instability (MSI, $p < 0.001$) and to be assigned as Consensus Molecular Subtype 1 (CMS1, $p < 0.001$) (Table 1). Additionally, patients with *BRAFMT* tumors were significantly more likely to be female ($p = 0.04$ and $p = 0.001$) and to receive no adjuvant chemotherapy ($p = 0.001$ and $p = 0.006$) compared to *KRASMT* and *WT/WT* respectively (Table 1). Finally, *BRAFMT* patients were significantly more likely to have later stage disease (stage II v III) compared to *WT/WT* patients ($p = 0.04$) (Table 1). Using the 64 gene *BRAF* classifier identified by Popovici *et al.* [7] we performed semi-supervised hierarchical clustering of the gene expression profiles of the entire stage II/III patient cohort. We identified a subgroup accounting for 28% ($n = 127$) of the tumor profiles using this method of clustering, which displayed an expression pattern similar to the pred-BRAFm profile (Supplementary Figure 2A). We found no difference in relapse rates between the pred-BRAFm and the pred-BRAFwt populations in this cohort (Supplementary Figure 2A; HR = 0.95 (95% CI 0.65–1.39)).

Gene expression associated with risk of relapse in BRAFMT CC

Gene Set enrichment analysis (GSEA) of the discovery subset indicated increased myogenesis, epithelial-to-mesenchymal transition (EMT) and hypoxia pathways in the *BRAFMT* tumors with the highest-risk of disease relapse (Supplementary Figure 2B). Additionally, using the Microenvironment Cell Populations-counter (MCP), we identified a non-significant trend for increased fibroblasts in high-risk *BRAFMT* tumors (Supplementary Figure 2C). Using differential gene expression analysis contrasting profiles from high-risk or low-risk *BRAFMT* tumors in the discovery subset (Supplementary Figure 1), we identified 83 probesets (Supplementary Table 1) corresponding to 67 annotated genes that are prognostic for relapse risk in *BRAFMT* tumors; high expression of 43 genes were associated with increased risk of relapse, and high expression of 24 genes with decreased risk of relapse (Table 2). Increased expression of endoplasmic reticulum stress-induced transcripts such as PPP1R15A (GADD34), heat shock proteins HSPA6 and DNAJB1,

Table 1: Characteristics of colon cancer patients and tumors according to BRAF and KRAS status.

Characteristic	BRAF MT *n* = 41	KRAS MT *n* = 166	*p*-value	WT/WT *n* = 210	*p*-value
Age, years, mean (SD)	76.0 (7.3)	67.7 (13.5)	<0.001	65.6 (12.6)	<0.001
Sex, *n* (%)					
Male	14 (34.1)	86 (51.8)		130 (61.9)	
Female	27 (65.9)	80 (48.2)	0.04	80 (38.1)	0.001
Tumour stage, *n* (%)					
II	20 (48.8)	86 (51.8)		138 (65.7)	
III	21 (51.2)	80 (48.2)	0.73	72 (34.3)	0.04
Tumour location, *n* (%)					
Proximal	37 (90.2)	86 (51.8)		49 (23.3)	
Distal	4 (9.8)	80 (48.2)	<0.001	161 (76.1)	<0.001
Adjuvant treatment* receipt, *n* (%)					
No	33 (80.5)	86 (51.8)		121 (57.6)	
Yes	8 (19.5)	80 (48.2)	0.001	89 (42.4)	0.006
MSI status					
MSI	27 (65.9)	15 (9.0)		15 (7.1)	
MSS	8 (19.5)	138 (83.1)		170 (81.0)	
Unknown	6 (14.6)	13 (7.8)	<0.001	25 (11.9)	<0.001
Consensus Molecular Subtype, *n* (%)					
CMS 1	32 (78.1)	17 (10.2)		26 (12.4)	
CMS 2	0 (0.0)	53 (31.9)		120 (57.1)	
CMS 3	3 (7.3)	35 (21.1)		9 (4.3)	
CMS 4	3 (7.3)	45 (27.1)		40 (19.1)	
Unknown	3 (7.3)	16 (9.6)	<0.001	15 (7.1)	<0.001

Characteristics of colon cancer patients and tumours according to BRAF and KRAS status.
MSI: Microsatellite instability; MSS: Microsatellite stable; MT: Mutant; WT/WT: BRAF and KRAS wild-type. *Adjuvant chemotherapy treatment receipt.
Of the 460 tumor profiles within our cohort, 417 have KRAS and BRAF mutational analysis data. Comparative analysis was performed for age, sex, stage, location, treatment, MSI and Consensus Molecular Subtype (CMS). MSI: Microsatellite instability; MSS: Microsatellite stable; MT: Mutant; WT/WT: BRAF and KRAS wild-type. *Adjuvant chemotherapy treatment received.

and the stress-related transcription factor DDIT3 were observed in *BRAFMT* tumours with the highest-risk of disease relapse.

While the majority of the 67 genes are represented by a single probeset, *BCL2L1* (encoding *Bcl-xL*) and *NCRNA00275* (which transcribes *ZFAS1*) are both represented by 3 *different* probesets (of the 4 total probesets for each gene), reducing the probability of the single genes themselves being false positives, which could potentially confound the validity of genes identified by a single probeset only (Supplementary Table 1). Gene expression levels of *Bcl-xL* were increased between 1.76–1.97 fold (Figure 1A) and *ZFAS1* by 1.83–1.90 fold (Supplementary Table 1) in the high-risk group compared to the low risk group. Importantly, the 67 *BRAFMT* prognostic gene list is distinct from the pred-BRAFm classifier reported by Popovici, as only one gene, (Kallikrein-Related Peptidase 10 (KLK10)), overlaps between these 2 gene lists (Supplementary Figure 2D).

Probesets associated with risk in BRAFMT tumors represent distinct novel prognostic biology

As *BRAF* and *KRAS* are both key components of the EGFR/MAPK pathway, we performed a similar risk association analysis in *KRASMT* tumors and identified 139 probesets associated with risk-of-relapse in this genetic subgroup (Supplementary Table 2). We found no overlap between the probesets associated with risk-of-relapse in the *KRASMT* subgroup and the probesets identified in the *BRAFMT* analyses (Supplementary Figure 2E), indicating that distinct biologies determine prognosis in these two subgroups, at least in stage II/III disease.

Table 2: Gene list associated with relapse in *BRAFMT* tumors

Symbol	Entrez Gene Name	Symbol	Entrez Gene Name
AEBP1	AE binding protein 1	AGR2	anterior gradient 2, protein disulphide isomerase family member
ALPP	alkaline phosphatase, placental	C2orf72	chromosome 2 open reading frame 72
ANGPTL1	angiopoietin-like 1	C3orf70	chromosome 3 open reading frame 70
BCL2L1	BCL2-like 1	COBL	cordon-bleu WH2 repeat protein
CCDC71L	coiled-coil domain containing 71-like	EFNA2	ephrin-A2
CCL7	chemokine (C-C motif) ligand 7	GATA6-AS1	GATA6 antisense RNA 1 (head to head)
CDA	cytidine deaminase	GMDS	GDP-mannose 4,6-dehydratase
CYSRT1	cysteine-rich tail protein 1	HES6	hes family bHLH transcription factor 6
DDIT3	DNA-damage-inducible transcript 3	IMPA2	inositol(myo)-1(or 4)-monophosphatase 2
DNAJB1	DnaJ (Hsp40) homolog, subfamily B, member 1	KIAA1324	KIAA1324
DNTTIP1	deoxynucleotidyltransferase, terminal, interacting protein 1	KIAA1671	KIAA1671
DUSP14	dual specificity phosphatase 14	KREMEN1	kringle containing transmembrane protein 1
EPYC	epiphycan	LARGE	like-glycosyltransferase
FST	follistatin	NOX1	NADPH oxidase 1
FXYD5	FXYD domain containing ion transport regulator 5	NRARP	NOTCH-regulated ankyrin repeat protein
GAS1	growth arrest-specific 1	PER2	period circadian clock 2
GJB3	gap junction protein, beta 3, 31kDa	PIP5K1B	phosphatidylinositol-4-phosphate 5-kinase, type I, beta
GJB5	gap junction protein, beta 5, 31.1kDa	PSMG4	proteasome (prosome, macropain) assembly chaperone 4
HCFC1R1	host cell factor C1 regulator 1 (XPO1 dependent)	SKP2	S-phase kinase-associated protein 2, E3 ubiquitin protein ligase
HSPA6	heat shock 70kDa protein 6 (HSP70B')	SLC22A23	solute carrier family 22, member 23
IER5L	immediate early response 5-like	SPRED2	sprouty-related, EVH1 domain containing 2
IGFBP6	insulin-like growth factor binding protein 6	TMEM30B	transmembrane protein 30B
KLK10	kallikrein-related peptidase 10	TRIM15	tripartite motif containing 15
KRT16	keratin 16, type I	TSPAN13	tetraspanin 13
MFGE8	milk fat globule-EGF factor 8 protein		
MIR100HG	mir-100-let-7a-2 cluster host gene		
MYH4	myosin, heavy chain 4, skeletal muscle		
NKIRAS1	NFKB inhibitor interacting Ras-like 1		
NPC1L1	NPC1-like 1		
NT5E	5'-nucleotidase, ecto (CD73)		
PAEP	progestagen-associated endometrial protein		
PDP1	pyruvate dehyrogenase phosphatase catalytic subunit 1		
PHLDA3	pleckstrin homology-like domain, family A, member 3		
PPP1R15A	protein phosphatase 1, regulatory subunit 15A		
PRR9	proline rich 9		
RBMS2	RNA binding motif, single stranded interacting protein 2		
RGS4	regulator of G-protein signaling 4		
TAGLN3	transgelin 3		
TGFB2	transforming growth factor, beta 2		
TNFSF4	tumor necrosis factor (ligand) superfamily, member 4		
VEGFB	vascular endothelial growth factor B		
ZFAS1	ZNFX1 antisense RNA 1		
ZNF667-AS1	ZNF667 antisense RNA 1 (head to head)		

Genes associated with increased (red) and decreased (green) relapse risk from our BRAFMT risk-supervised differential gene expression analysis data.

Bcl-xL mRNA expression is associated with poor prognosis in stage II/III BRAFMT CC

To confirm the clinical relevance of elevated *Bcl-xL* gene expression in our training set, in addition to testing the genotype-specific nature of its prognostic value, we next generated an "Initial Consolidation" dataset (n = 417, Supplementary Figure 1) by removing the filters initially applied to the discovery subset of the GSE39582 cohort, (i.e. we removed the restrictions on chemotherapy treatment and the follow-up criteria as detailed in Methods). This set of 417 patients represents an ideal cohort to assess the prognostic value of *Bcl-xL* in *KRASWT* and *WT/WT* patients that were not used to identify *Bcl-xL,* in addition to a further 17 *BRAFMT* patients that were previously excluded from the discovery data. Within *BRAFMT* tumors (n = 41), the *Bcl-xL*-high group (*Bcl-xL*^{high}) had a significantly higher risk-of-relapse compared to the *Bcl-xL*-low (*Bcl-xL*^{low}) expression group, using either an unadjusted (HR = 5.83), or adjusted model (HR = 9.63) accounting for potential confounding factors including age, gender, TNM stage and MSI status (confidence intervals could not be calculated due to an absence of events in *Bcl-xL*^{low}; Figure 1B and Table 3). When examining untreated patients only, the prognostic value of *Bcl-xL* mRNA expression in *BRAFMT* patients was again apparent (Figure 1C); however, the prognostic value of *Bcl-xL* in the chemotherapy-treated patient subgroup could not be evaluated due to small numbers (n = 8). The *Bcl-xL* medium expression group (*Bcl-xL*^{med}) displayed an intermediate relapse profile compared to the *Bcl-xL*^{high} and *Bcl-xL*^{low}, suggesting a dose-response association between relapse risk and *Bcl-xL* gene expression. Stratification based on the median also demonstrated the prognostic value of *Bcl-xL* gene expression (HR = 5.24 (95% CI 1.3–21.2)) (Supplementary Figure 3A).

In contrast, although there was a suggestive prognostic trend, no significant associations were observed for *Bcl-xL* gene expression in either the *KRASMT* or *WT/WT* patient groups, using either an adjusted or unadjusted analysis model (Table 3 and Supplementary Figure 3B and 3C).

ZFAS1 mRNA expression is associated with poor prognosis in stage II/III BRAFMT CC

High gene expression of *ZFAS1* was associated with a prognostic trend in *BRAFMT* tumors compared to low gene expression (Supplementary Figure 4A) although given the small number of events in this stratified group, this trend failed to reach significance in either unadjusted

A

Probe ID	Gene Symbol	p-value	Fold-Change
212312_at	BCL2L1 (Bcl-xL)	0.0025	1.76
206665_s_at	BCL2L1 (Bcl-xL)	0.0040	1.84
215037_s_at	BCL2L1 (Bcl-xL)	0.0019	1.97

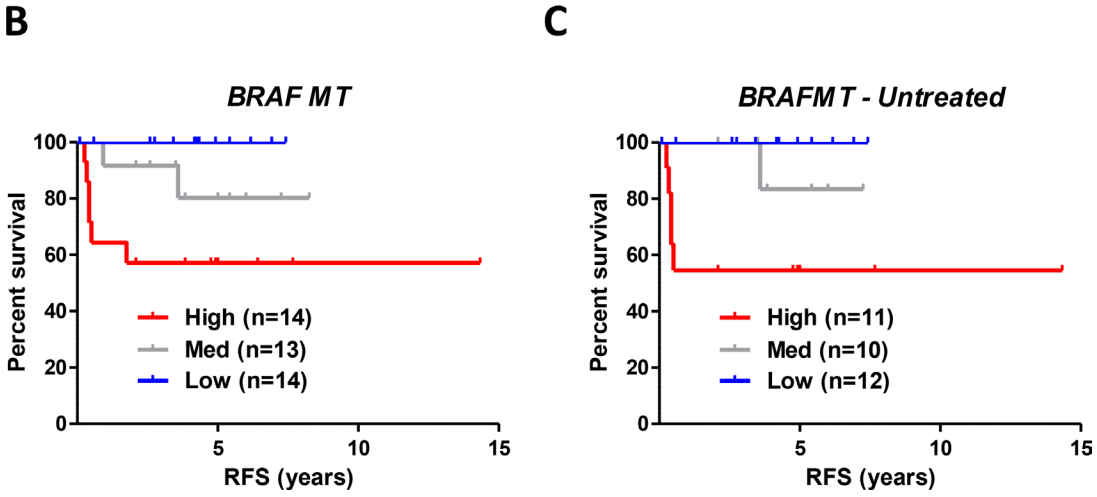

Figure 1: Relapse risk analysis of *BRAFMT* tumors indicates that *Bcl-xL* gene expression is associated with prognosis in *BRAFMT* tumors. (**A**) BCL2L1 (*Bcl-xL*) was represented by 3 individual probesets in relapse risk analysis in *BRAFMT* tumors. (**B** and **C**) Relapse-free survival (RFS) curve using Kaplan-Meier estimation in the "Initial Consolidation" dataset comparing tertile stratified *Bcl-xL* gene expression levels in all *BRAFMT* (A) and untreated *BRAFMT* (B) stage II/III CRC patients. Unadjusted and adjusted HR statistics are detailed in Table 3.

Table 3: Unadjusted and adjusted analyses of relapse-free survival

Bcl-xL	Non-progressors *n*	Progressors *n*	Unadjusted Hazard ratios (95% confidence intervals)	Adjusted** Hazard ratios (95% confidence intervals)
BRAF MT				
Low	14	0	1.00	1.00
Medium	11	2	1.80 (Not calculable)	3.94 (Not calculable)
High	8	6	5.83 (Not calculable)	9.63 (Not calculable)
KRAS MT				
Low	38	18	1.00	1.00
Medium	33	21	1.45 (0.75–2.77)	1.47 (0.76–2.84)
High	34	22	1.25 (0.65–2.40)	1.32 (0.68–2.56)
WT/WT				
Low	57	13	1.00	1.00
Medium	53	17	1.39 (0.67–2.85)	1.27 (0.61–2.64)
High	50	20	1.54 (0.77–3.10)	1.47 (0.72–3.01)

MT: Mutant; WT/WT: BRAF and KRAS wild-type.
*Cut-offs for low/medium/high Bcl-xl gene expression based on tertile values within each BRAF/KRAS status subgroup.
**Adjustments included age and sex, and were tested for TNM stage, MSI status, adjuvant chemotherapy receipt and tumour location for all models. A backwards elimination model was applied for tested confounders until all were significant at the $p < 0.25$ level in the model. Final adjustments included age, sex, TNM stage and MSI status (for BRAF MT and WT/WT); age, sex, TNM stage, adjuvant chemotherapy receipt and tumour location (for KRAS MT).
RFS analysis was performed using Cox proportional hazards method in the *BRAFMT, KRASMT* or *WT/WT* stratified by *Bcl-xL* expression levels. Analysis was performed both before and following adjustment. *Cut-offs for low/medium/high *Bcl-xL* gene expression based on tertile values within each BRAF/KRAS status subgroup. **Adjustments included age and sex, and were tested for TNM stage, MSI status, adjuvant chemotherapy receipt and tumor location for all models. A backwards elimination model was applied for tested confounders, until all were significant at the $p < 0.25$ level in the model. Final adjustments included age, sex, TNM stage and MSI status (for BRAF MT and WT/WT); age, sex, TNM stage, adjuvant chemotherapy receipt and tumor location (for KRAS MT).

HR = 4.69 (95% CI 0.52–42.01), or adjusted HR = 4.71 (95% CI 0.50–44.00) analyses (Supplementary Table 3). There was no prognostic value associated with high *ZFAS1* expression in the *KRASMT* population (adjusted HR = 0.65 (95% CI 0.34–1.24)), although there was a significant association with lower relapse rates in the WT/WT population (adjusted HR = 0.47 (95% CI 0.24–0.92)) (Supplementary Figure 4B, Supplementary Table 3) indicating an opposing prognostic role in these distinct tumor genotypes.

Bcl-xL gene and protein expression are associated with the epithelial component of the tumor

Given the multiple cell types that constitute the tumor microenvironment (TME) in CC, we analyzed *Bcl-xL* mRNA expression levels in transcriptional data derived from micro-dissected tumor tissue (detailed in Materials and Methods section). We observed that its expression was bimodal in the epithelial compartment of the TME, with high and low subgroups around the median, whereas stromal expression levels were generally low, with values below the median (Supplementary Figure 5A). Analysis of matched Bcl-xL transcript abundance (by Agilent microarray), and protein level, (by Reverse Phase Protein Array (RPPA)) from 102 CRC tumor samples within The Cancer Genome Atlas (TCGA) indicated a significant correlation between both methodologies ($p = 0.001$; Supplementary Figure 5B), supporting protein-based assessment as an appropriate methodology to validate our data in an independent cohort. Following optimization of an IHC protocol for *Bcl-xL* protein expression, the predominantly epithelial-derived nature of *Bcl-xL* protein expression and neoplastic-specific staining compared to the normal glands in surrounding tissue was confirmed in a series of whole-face CC sections, although there does appear to be some stromal expression, in line with our transcriptional analysis (Figure 2A).

Independent validation of Bcl-xL as a poor prognostic marker specifically in stage II/III BRAFMT CC

We then independently validated the prognostic value of *Bcl-xL* protein expression specifically in *BRAFMT*

patient samples from within a Northern Ireland cohort (n = 661) (Supplementary Figure 1 and described in Methods). Employing tertiles defined by protein expression (Figure 2B), we found that *Bcl-xL*^{high} was associated with an increased risk of CRC disease-specific survival (DSS; n = 77) when compared with *Bcl-xL*^{low}, in both unadjusted (HR = 3.07 (95% CI 1.24–7.60)) and adjusted models (HR = 5.50 (95% CI 1.71–17.69) (Supplementary Figure 6A and Table 4). Similar findings were evident when using OS (n = 92) as the endpoint (Supplementary Figure 6B).

We next conducted stratified analyses within the Northern Ireland cohort to assess independently the prognostic value of Bcl-xL protein expression in both untreated and chemotherapy-treated *BRAFMT* patients. In untreated patients, we observed a 12-fold increased DSS risk in patients with the highest Bcl-xL protein expression (adjusted model HR = 12.13 (95% CI 2.49–59.13)) (Figure 3A), which was not observed in treated patients, (adjusted model HR = 0.96 (95% CI 0.08–11.42)) (Supplementary Figure 6C and Table 4). This significant

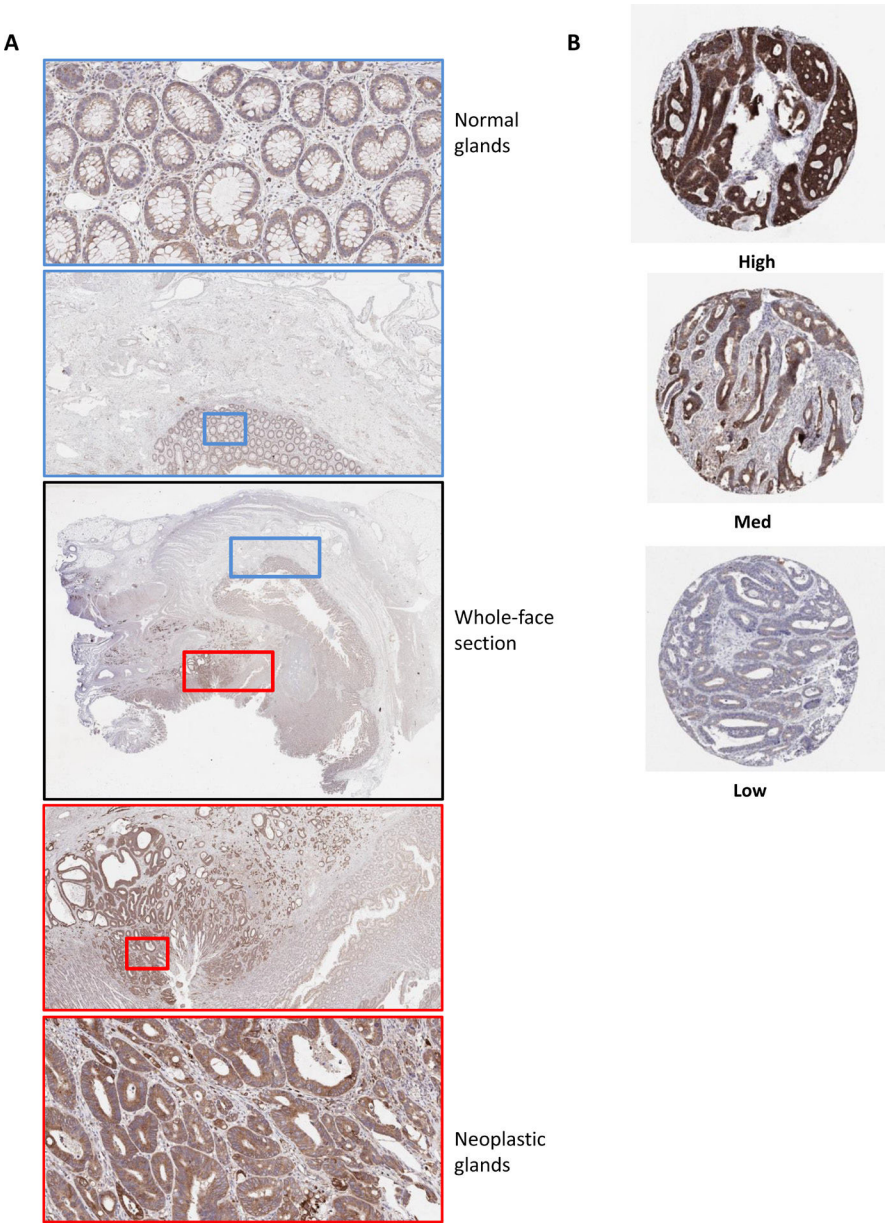

Figure 2: Optimization of immunohistochemistry staining protocol for Bcl-xL protein expression in CC. (**A**) Whole-face CC tissue sections were used to optimize IHC protocol. A low level of protein expression was observed in the normal glands compared to surrounding stroma (Blue box) Elevated levels of expression were observed in neoplastic glands compared to both the normal glands and surrounding stroma (Red box). Some staining in the stroma is evident in both normal and cancer-associated regions. (**B**) Representative images of high, medium and low Bcl-xL protein expression by IHC in an independent "Northern Ireland cohort" of stage II/III CRC (Northern Ireland cohort; n = 740).

Table 4: Analyses of disease-specific survival in the independent IHC validation cohort

Bcl-xL	Alive *n*	CRC Death (DSS) *N*	Unadjusted Hazard ratios (95% confidence intervals)	Adjusted** Hazard ratios (95% confidence intervals)
BRAF MT				
Low (<56.1)	16	7	1.00	1.00
Medium (56.1–<91.1)	17	10	1.54 (0.58–4.09)	1.97 (0.60–6.44)
High (≥91.1)	12	15	3.07 (1.24–7.60)	5.50 (1.71–17.69)
KRAS MT				
Low (<53.5)	44	28	1.00	1.00
Medium (53.5–<92.7)	41	24	0.98 (0.57–1.69)	0.93 (0.52–1.66)
High (≥92.7)	38	33	1.37 (0.82–2.27)	1.00 (0.57–1.77)
WT/WT				
Low (<66.1)	57	28	1.00	1.00
Medium (66.1–<105.8)	58	29	0.99 (0.59–1.68)	1.05 (0.60–1.84)
High (≥105.8)	59	31	1.07 (0.64–1.78)	1.18 (0.67–2.09)

MT: Mutant; WT/WT: BRAF and KRAS wild-type.
*Cut-offs for low/medium/high Bcl-xl gene expression based on tertile values within each BRAF/KRAS status subgroup.
**Adjustments included age, sex, TNM stage, MSI status, adjuvant chemotherapy receipt, ECOG status, family history of colorectal cancer, year of diagnosis and extramural venous invasion for all models.

Bcl-xL	No Chemotherapy receipt			Chemotherapy receipt		
	Alive *n*	CRC Death (DSS) *N*	Adjusted Hazard ratios (95% confidence intervals)	Alive *n*	CRC Death *n*	Adjusted Hazard ratios (95% confidence intervals)
BRAF MT						
Low (<56.1)	11	4	1.00	5	3	1.00
Medium (56.1–<91.1)	12	6	1.99 (0.38–10.29)	5	4	2.18 (0.23–20.89)
High (≥91.1)	3	12	12.13 (2.49–59.13)	9	3	0.96 (0.08–11.42)
P for interaction			0.006			

MT: Mutant.
Cut-offs for low/medium/high Bcl-xl gene expression based on tertile values within each BRAF MT subgroup.
Adjustments included age, sex, TNM stage, MSI status, adjuvant chemotherapy receipt, ECOG status, family history of colorectal cancer, year of diagnosis and extramural venous invasion.
(Top) DSS analysis was performed using Cox proportional hazards method in the *BRAFMT*, *KRASMT* or *WT/WT* stratified by Bcl-xL IHC (H-score) protein expression levels. Analysis was performed both before and following adjustment.
*Cut-offs for low/medium/high *Bcl-xL* gene expression based on tertile values within each BRAF/KRAS status subgroup.
**Adjustments included age, sex, TNM stage, MSI status, adjuvant chemotherapy receipt, ECOG status, family history of colorectal cancer, year of diagnosis and extramural venous invasion for all models. (Bottom) Further adjusted analysis to identify treatment interaction effect of the Bcl-xL-high tertile group of BRAFMT tumors stratified by treatment received.

prognostic benefit from adjuvant chemotherapy in *BRAFMT* patients was only observed in patients with the highest Bcl-xL protein expression (*P*-value for interaction = 0.006), whereas patients with low Bcl-xL protein expression derived no benefit from the addition of chemotherapy (Figure 3B and 3C, Table 4 and Supplementary Figure 6C). Similar results were evident when using OS as the endpoint (Supplementary Figure 6D–6F). Importantly, in agreement with our initial consolidation cohort, we were again able to confirm that the prognostic value of Bcl-xL protein expression was not observed in *KRASMT* (HR = 1.00 (95% CI 0.57–1.77) and *WT/WT* (HR = 1.18 (95% CI 0.67–2.09)) patient samples (Table 4).

DISCUSSION

In this study, we set out to identify factors influencing patient prognosis specifically in tumors harboring an oncogenic *BRAF* mutation. Stratification of a discovery prognostic cohort based on risk-of-relapse identified the *Bcl-2* family member, *Bcl-xL*, as being upregulated at the transcriptional level in *BRAF*MT tumors from patients who went on to relapse following surgery, compared to those *BRAFMT* patients who experienced no disease recurrence. We validated the prognostic value of *Bcl-xL* specifically in *BRAFMT* tumors in both a consolidation transcriptional cohort and in an independent

population-based stage II/III cohort. Importantly, in each validation series, we also confirmed the *BRAFMT*-specific nature of this association, as in either *KRASMT* or *WT/WT* tumors, the expression of *Bcl-xL* was not associated with increased risk of disease relapse or death. Interestingly, we observed that although *BRAFMT* tumors with high *Bcl-xL* expression have a poor prognosis, this subgroup also appears to benefit the most from standard adjuvant chemotherapy.

The prognostic value of stratifying CC patients based on *BRAF* mutational status has been well reported, particularly in stage IV metastatic tumors, where patients with *BRAFMT* tumors have poor survival rates. A previous study identified a transcriptional signature that could stratify stage II and III CRC tumor profiles into subgroups based on their similarity to *BRAFMT* tumors (pred-BRAFm) [7]. The authors demonstrated the utility of either *BRAF* mutational status or the pred-BRAFm classifier in identifying patients with shorter survival, although no difference was observed in the initial disease-specific relapse rates between the identified subgroups. This important result suggests that the prognostic power associated with the pred-BRAFm signature, or indeed the presence of the *BRAF* mutation itself, is due to shorter survival time because of aggressive disease *after* relapse in stage IV disease; however, initially, *BRAFMT* stage II and III patients are not at a higher risk of their early-stage disease progressing to metastatic disease. This subtle but crucial point underpins our rationale for performing a stratified analysis to identify factors determining risk-of-relapse specifically *within* the *BRAFTMT* genotype. The data presented here identifies for the first time a novel role for *Bcl-xL* expression in influencing disease relapse, providing a new, important and clinically relevant understanding of the biology underpinning aggressive *BRAFMT* stage II/III disease. Interestingly, we found almost no overlap between the genes associated with relapse in *BRAFMT* and *KRASMT* tumors, suggesting that although there is constitutive activation of the MAP kinase pathway in both these subgroups, there is clearly distinct prognostic tumor biology associated with these different genotypes.

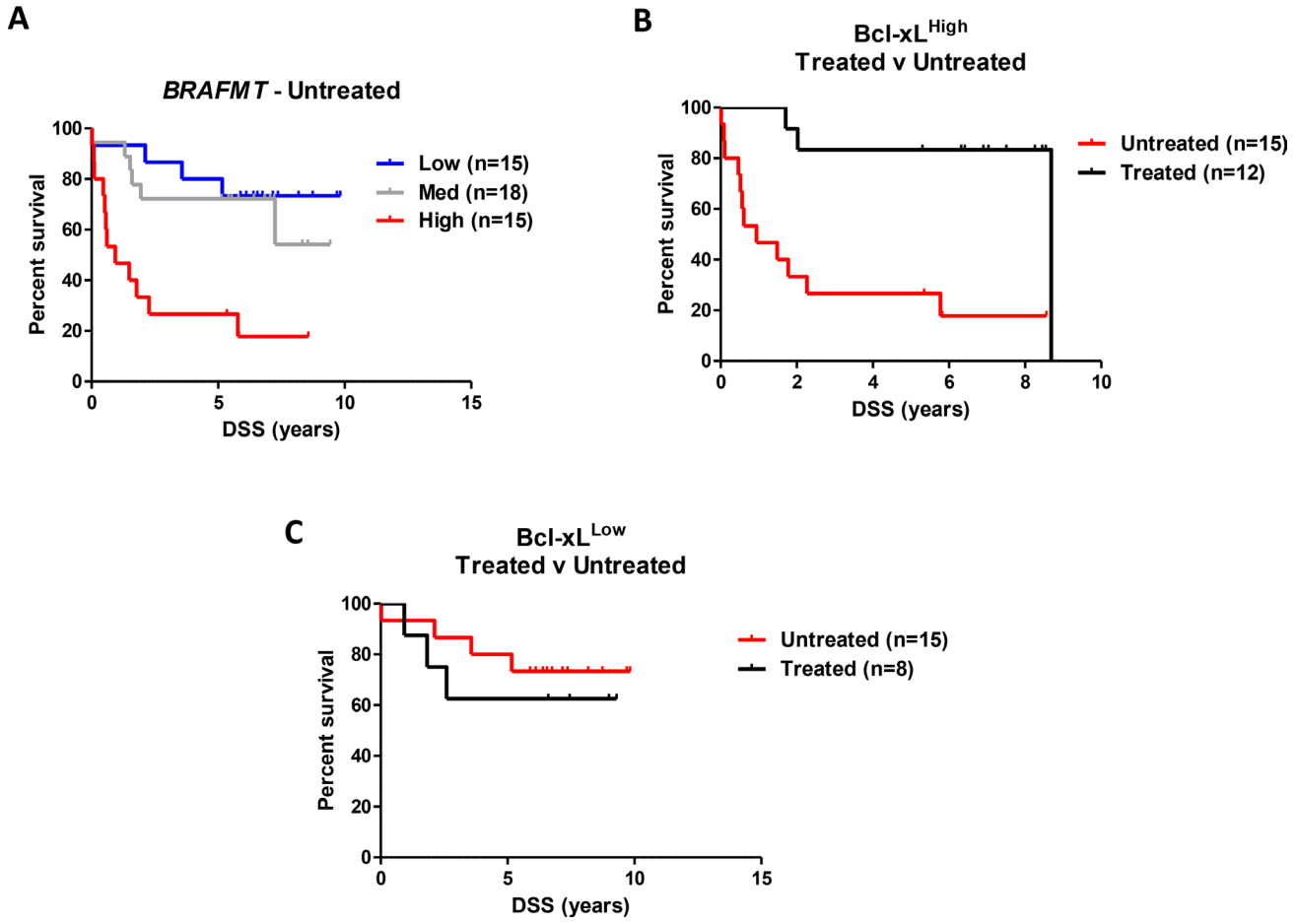

Figure 3: Independent validation of the prognostic value of Bcl-xL protein expression in *BRAFMT* CC. (**A**) Colorectal cancer disease-specific survival (DSS) curve using Kaplan-Meier estimation in the "Northern Ireland cohort" comparing tertiles stratification of *Bcl-xL* protein expression (by IHC H-score) in untreated *BRAFMT* stage II/III CC patients. (**B**) DSS of patients in the highest tertile of *Bcl-xL* protein expression stratified according to adjuvant chemotherapy treatment received. (**C**) DSS of patients in the lowest tertile of *Bcl-xL* protein expression stratified according to adjuvant chemotherapy treatment received. Unadjusted and adjusted HR statistics are detailed in Table 4.

The benefits of combining transcription-array discovery followed by IHC validation in independent patient cohorts, as we have employed in our study, was recently demonstrated in an analysis of stage II/III CC to identify a subgroup of undifferentiated tumors characterized by poor differentiation and low expression of the transcription factor *CDX2* [8]. There are a number of parallels between the *CDX2* study and our own, as they both use exploratory and retrospective analysis followed by clinically relevant IHC biomarker validation to identify a small subgroup of stage II/III patients with poor prognosis that appear to respond to adjuvant chemotherapy. Poorly differentiated tumors have previously been associated with right-sided MSI, CIMP disease [9]; however, the prognostic value of *BRAF* mutation was shown to be independent of *CDX2* expression [10]. Our analysis did not identify *CDX2* gene expression as a driver of disease relapse specifically in *BRAFMT* tumors and reciprocally *Bcl-xL* was not identified as prognostic across the entire CC population in the *CDX2* study (similar to our data in *BRAFWT* tumors), thus suggesting that we have identified a unique subgroup of poor prognostic patients. However, as the *CDX2* study did not collect or utilize *BRAF* mutation status, this could not be further assessed using their data.

A previous study of Bcl-xL protein expression in CRC determined that high expression of this biomarker was associated with poor prognosis across the entire patient cohort [11]. Importantly, this data indicated a potentially confounding variable, as increased Bcl-xL expression was also significantly associated with later stage disease (already a well-established prognostic factor) [12]. In agreement with this earlier study, we also found that Bcl-xL expression was associated with later stage disease; however, using an adjusted analysis to take into account known confounding clinical factors (including stage), we show that Bcl-xL expression can independently predict prognosis, but only in *BRAFMT* tumors. A recent study using RPPA methodology reported that a mathematical model of Bcl-2 family protein interactions (including Bcl-xL) termed DR_MOMP was prognostic in chemotherapy-treated stage III CRC [13]. Moreover, this study found that Bcl-2 family signaling was particularly important in Consensus Molecular Subtypes (CMS) 1 and 3. As the CMS1 subgroup is enriched for *BRAFMT* disease, this report appears to be in agreement with our current study. However, the individual contribution of Bcl-xL expression to prognosis in CMS1/*BRAFMT* CRC was not reported; the study may have been underpowered in that respect.

The reason for the significant benefit from standard chemotherapy of Bcl-xL high *BRAFMT* CRC is unclear. High Bcl-xL expressing tumors may be "primed" to undergo apoptosis in response to chemotherapy, due to co-expression of pro-apoptotic Bcl-2 family members. [14, 15] A recent high-throughput drug screen aimed at uncovering therapeutic strategies in CRC, revealed the essentiality of MCL1, Bcl-2 and Bcl-xL in *BRAFMT*-driven disease [16]. Additionally, a further drug screening-based study identified Bcl-xL as a critical regulator of MEK inhibitor resistance, which was synthetically lethal across a broad panel of *BRAFMT* cell line models [17]. These findings and the findings presented in our study suggest that directly targeting Bcl-xL may be an effective therapeutic strategy for *BRAFMT* CRC in the adjuvant disease setting.

We also identified high expression of the long noncoding RNA *ZFAS1* as a poor prognostic marker in our discovery dataset. *ZFAS1* was previously reported to be overexpressed in CRC compared to adjacent non-CRC tissue, with siRNA-mediated targeting revealing its role as a regulator of p53 protein levels, cell proliferation and colony formation in a small panel of CRC cell lines [18]. Validation of this marker, using methodologies such as RNA *in situ* hybridization, may clarify its role in disease progression and may become increasingly important as our understanding of the biology of long noncoding RNAs increases.

The findings presented both here and by others suggest that *BRAFMT* driven CRC is more aggressive than *BRAFWT* disease, but only when the disease has disseminated from the primary site. Interestingly, we observed specific changes in the ER-stress machinery in *BRAFMT* tumors with the highest-risk of disease relapse, with activation and upregulation of factors including GADD34, heat shock proteins, and stress-related transcription (DDIT3) in our analysis. Additionally, using GSEA, we identify increased hypoxia and EMT signaling in high-risk tumors, again indicating an association with ER stress-activation. Each of these factors have been demonstrated to activate the unfolded protein response (UPR), which in turn has been correlated with a higher risk of metastatic recurrence in breast cancer [19, 20]. In agreement with our findings, upregulation of UPR signaling in disseminated tumor cells from breast cancer, lung cancer and prostate cancer enables both the formation and long term persistence of metastatic lesions [19, 20]. In addition to activation of the UPR machinery, high Bcl-xL expression may promote survival of invasive tumor cells during the metastatic process; for example Bcl-xL has been reported to be a suppressor of anoikis, [15, 21] which would explain its association with increased risk-of-relapse in the *BRAFMT* subgroup.

This study has several strengths. We have identified Bcl-xL as a novel predictor of response within a poor prognostic group of CC patient samples, using a robust approach that included validation in an independent cohort using a clinically relevant methodology. Importantly, while we do find significant prognostic and predictive value using Bcl-xL gene expression in 2 independent cohorts, final validation of this discovery approach would require transcriptional data, detailed treatment information and clinical follow up from an independent well balanced cohort, preferably in a clinically trial setting, enriched

for the specific subtype of interest, in our case *BRAFMT* stage II/III CRC. The population-based nature of our validation cohort also means that the results should be generalizable to all stage II/III CRC patients, however we do acknowledge that by using a population-based approach for validation of these findings, there may be a selection bias for patients who subsequently received chemotherapy, and this that may have impacted on our results. Additionally, given that IHC and mutational tests for *BRAF* and *KRAS* are routinely utilized in the diagnostic work-up of CC patients, the methods we have used here could easily be employed within routine pathology reporting practice. However, we do acknowledge that further work is required to identify an optimal cut-off level of *Bcl-xL* expression that would allow a more robust classification of low and high expressers for prospective patient stratification.

In conclusion, we have identified and independently validated the prognostic value of Bcl-xL mRNA and protein expression specifically within *BRAFMT* CC, which should help inform selection of treatment options for high-risk *BRAFMT* stage II/III patients in the adjuvant disease setting. This approach could prevent the initial relapses, which ultimately contribute to the poor outcomes of patients with this genotype. Data presented here provide compelling evidence that, in addition to *BRAF* mutational analysis, assessment of Bcl-xL protein expression using routine diagnostic IHC methods can identify both poor prognostic *BRAFMT* stage II/III CC patients who will benefit from adjuvant therapy and an otherwise good prognostic subgroup of *BRAFMT* patients who derive no significant advantage from the addition of adjuvant chemotherapy.

MATERIALS AND METHODS

Transcriptional datasets

Gene expression profiles were downloaded from NCBI Gene Expression Omnibus (GEO) (http://www.ncbi.nlm.nih.gov/geo/). Accession number GSE39582 contains 566 tumor transcriptional profiles (460 stage II/III) from a CC series and has previously been employed by the CRC subtyping consortium [22, 23]. As detailed in Supplementary Figure 1, the GSE39582 cohort contained 460 stage II/III CC profiles which had relapse data available. For initial biomarker discovery, the "Prognostic Subset" contained untreated stage II/III patients stratified into high-risk (if the patient relapsed within 36 months) or low-risk (if there was no relapse). The "Initial Consolidation" contained all stage II/III patients with relapse information and mutational data (n = 417), which included *BRAFMT* (n = 41; 24 of which will have been used already in the prognostic subset), *KRASMT* (n = 166) or *WT/WT* (n = 210) (Supplementary Figure 1). Accession number GSE35602 contains profiles from 13 CRC cases, which were obtained using laser-microdissected tissue to extract RNA specifically from stroma or epithelium regions separately, followed by gene expression microarray analysis.

Transcriptomics (Agilent; mRNA_Preprocess_Median) and protein (Reverse Phase Protein Array/mda_rppa_core-protein_normalization) data were downloaded from the COAD pipeline in Firehose (https://gdac.broadinstitute.org/). Patient samples which had both mRNA and RPPA data were collated (n = 102) and were analysed with the Pearson's correlative analysis using GraphPad Prism version 5 for Windows.

Transcriptional analysis

Partek Genomics Suite was employed for dataset analysis. Differentially expressed probesets which had a fold-change +/– 1.75 fold and p-value < 0.005 were defined using analysis of variance (ANOVA) of supervised risk groupings in both the *BRAFMT* and *KRASMT* subgroups separately. Genes represented three times by different probesets were selected for further genotype-specific survival analysis. This method inevitably increases false negatives, by ruling out genes represented by fewer probesets, but it increases the confidence in the positive results. In the *BRAFMT* analysis, these criteria identified *BCL2L1* (*Bcl-xL*) and *NCRNA00275* (*ZFAS1*). Gene Set Enrichment Analysis was accessed (GSEA; http://software.broadinstitute.org/gsea/index.jsp) and the Microenvironment Cell Populations-counter (MCP) was accessed via the https://doi.org/10.5281/zenodo.61372 link.

Bcl-xL Immunohistochemistry (Bcl-xL IHC)

We optimized a protocol for Bcl-xL IHC on sections of CRC tissue using various antibody dilutions and processing parameters. In line with REMARK guidelines, reproducibility and robustness were tested using a TMA block containing 20 cores of CRC tumor from different patient resections. For staining of the control and independent cohort TMAs, sections were cut at 4 μm on a rotary microtome, dried at 37° C overnight, and then used for IHC, which was performed on an automated immunostainer (Leica Bond-Max, Milton Keynes, UK). Antigen-binding sites were detected with a polymer-based detection system (Bond, Newcastle Upon Tyne, UK; cat. no. DS9800). *Bcl-xL* IHC antibody (Cell Signaling Technology, MA, United States) (*Bcl-xL* (54H6) Rabbit mAb #2764) was employed at 1:250 dilution with epitope retrieval solution 2 pretreatment for 30 minutes. All sections were visualized with diaminobenzidine, counterstained with hematoxylin, and mounted in DPX.

Independent stage II/III CC Northern Ireland validation cohort

Candidate biomarkers identified from transcriptional datasets were then evaluated within a Northern Ireland

population-based cohort of stage II/III CC patient samples (n = 740) using immunohistochemical methods. The Northern Ireland Cancer Registry was used to identify all patients who underwent surgery in Northern Ireland between 2004 and 2008, for a single, primary, stage II or III colon adenocarcinoma (n = 1,539). A detailed clinical case note review was then conducted, to verify diagnosis and stage and to extract clinical information, including the use of adjuvant chemotherapy and outcome data. Following this review, n = 113 cases were excluded (7%), mainly on the basis of inaccurate staging. Of the remaining n = 1,426 patients, n = 740 patients (52%) were diagnosed within the jurisdiction of the Northern Ireland Biobank, of which specimens relating to n = 661 patients (89%) were successfully retrieved. All patients were followed up for occurrence and cause of death via linkage to the Northern Ireland Registrar General's Office, up to 31st December 2013. Patients were recorded as having a CRC-specific death if any cause of death was listed as ICD-codes C18, C19, C20 and/or C26.

Northern Ireland cohort immunohistochemical and mutational analysis

This cohort was assembled into a tissue microarray, containing 3 cores from epithelial-rich tumor regions per patient. Blocks were retrieved and tumor regions were annotated for subsequent coring (KA, MBL, JJ). One millimeter diameter tissue cores were extracted from donor blocks and inserted into recipient blocks using a manual tissue arrayer (Estigen, Tartu, Estonia). Additionally, mutational analysis was undertaken for KRAS and BRAF on n = 661 (89%) of the TMA cohort using the ColoCarta panel (Agena Bioscience, Hamburg, Germany). This panel includes: BRAF: D594V, V600E, V600K, V600L, V600R. HRAS Q61L. KRAS: A59T, G12A, G12C, G12D, G12F, G12R, G12S, G12V, G13D, G61H, Q61L. Following sequencing, mutational status of *BRAF* and *KRAS* was available for a sub-cohort (n = 661; *BRAFMT* n = 92, *KRASMT* n = 248, *WT/WT* n = 321). Using the IHC methodology optimized in line with the REMARK guidelines in whole face CC sections, we assessed *Bcl-xL* protein expression using digital pathology software, QuPath [24], to give a numerical representation of both the extent and the intensity of staining (H-score), based on the mean expression of all cores (3 cores for each patient). In line with REMARK guidelines, all scoring was performed while blinded to the clinical details of the cohort and the survival endpoints. Using tertile stratification methodology, we assigned patients in each mutational genotype into high, medium or low groups according to their Bcl-xL protein expression H-score.

Ethical approval

Clinical note review was conducted under the auspices of the Northern Ireland Cancer Registry ethical approval from ORECNI (REC: 10/NIR02/53). Ethical (REC:11/NI/0013, project NIB13-0069) and Bcl-xL staining (NIB16-0212) approval was received from the Northern Ireland Biobank.

Statistical analysis

Clinical characteristics were compared using chi-squared tests, according to mutational groupings. Tertile stratification in GSE39582 was performed on the mean biomarker, BCL2L1 (*Bcl-xL*), expression value from the three probesets used within the *BRAFMT* (n = 42), *KRASMT* (n = 166) and the *WT/WT* (n = 210) subgroups. Similarly, in the Northern Ireland cohort, tertile stratification was performed on the mean *Bcl-xL* H-score expression value from the multiple tumor cores available (up to 3 per patient) within the *BRAFMT* (n = 92), *KRASMT* (n = 248) and the *WT/WT* (n = 321) subgroups. Cox Proportional hazards analysis was conducted for both the transcriptional dataset and Northern Ireland cohort, prior to and after adjustment for potential confounders, to evaluate the association between *Bcl-xL* and survival in CC patients, according to *BRAF* and *KRAS* mutation status (Stata version 11.2, StataCorp, College Station, TX, USA).

Author contributions

PDD: Design of the study, data acquisition and analysis, interpretation of results, drafting the work and study supervision; HGC: Data acquisition and analysis, interpretation of results and revision of article; PB, MA: Data acquisition and analysis; RTG: Data acquisition, interpretation of results, collection of samples; SMcQ, VB, MBL, JAJ: Collection of samples; AMBMcC, AG, DK: Data analysis; CH, FDiN, ST: Interpretation of results; DMcA, PGJ, DBL: Study supervision, interpretation of results ; ML: Design of the study, interpretation of results, revision of article, study supervision and funding. All authors approved the final version of the submitted work.

ACKNOWLEDGMENTS

The samples used in this research were received from the Northern Ireland Biobank which is funded by HSC Research and Development Division of the Public Health Agency in Northern Ireland and Cancer Research UK through the Belfast CR- UK Centre and the Northern Ireland Experimental Cancer Medicine Centre; additional support was received from the Friends of the Cancer Centre. The Northern Ireland Molecular Pathology Laboratory which is responsible for creating resources for the NIB has received funding from Cancer Research UK, the Friends of the Cancer Centre and the Sean Crummey Foundation. The Northern Ireland Cancer Registry is funded by the Public Health Agency, Northern Ireland. We also thank Ken Arthur (Belfast) for his expertise in TMA construction of the

cohort, Enzo Medico (Torino) for his advice and expertise, and all individuals who were involved in the creation and study design of the Northern Ireland cohort.

CONFLICTS OF INTEREST

None.

FUNDING SUPPORT

This work was supported by The Entwistle Family Travel Award (PDD), a CRUK Population Research Fellowship (HGC), a CRUK Research Bursary (RG), a CRUK studentship (AMBMcC) a HSC R&D Fellowship (RG), a CRUK Programme Grant (PGJ) and a joint CRUK-MRC Stratified Medicine Programme Grant (S:CORT; PDD, MA, PGJ, ML).

Editorial note

This paper has been accepted based in part on peer-review conducted by another journal and the authors' response and revisions as well as expedited peer-review in Oncotarget.

REFERENCES

1. Mitsudomi T, Yatabe Y. Epidermal growth factor receptor in relation to tumor development: EGFR gene and cancer. FEBS J. 2010; 277:301–08. https://doi.org/10.1111/j.1742-4658.2009.07448.x.
2. Mao C, Wu XY, Yang ZY, Threapleton DE, Yuan JQ, Yu YY, Tang JL. Concordant analysis of KRAS, BRAF, PIK3CA mutations, and PTEN expression between primary colorectal cancer and matched metastases. Sci Rep. 2015; 5:8065. https://doi.org/10.1038/srep08065.
3. Maughan TS, Adams RA, Smith CG, Meade AM, Seymour MT, Wilson RH, Idziaszczyk S, Harris R, Fisher D, Kenny SL, Kay E, Mitchell JK, Madi A, et al, and MRC COIN Trial Investigators. Addition of cetuximab to oxaliplatin-based first-line combination chemotherapy for treatment of advanced colorectal cancer: results of the randomised phase 3 MRC COIN trial. Lancet. 2011; 377:2103–14. https://doi.org/10.1016/S0140-6736(11)60613-2.
4. Chapman PB, Hauschild A, Robert C, Haanen JB, Ascierto P, Larkin J, Dummer R, Garbe C, Testori A, Maio M, Hogg D, Lorigan P, Lebbe C, et al, and BRIM-3 Study Group. Improved survival with vemurafenib in melanoma with BRAF V600E mutation. N Engl J Med. 2011; 364:2507–16. https://doi.org/10.1056/NEJMoa1103782.
5. Kopetz S, Desai J, Chan E, Hecht JR, O'Dwyer PJ, Maru D, Morris V, Janku F, Dasari A, Chung W, Issa JP, Gibbs P, James B, et al. Phase II Pilot Study of Vemurafenib in Patients With Metastatic BRAF-Mutated Colorectal Cancer. J Clin Oncol. 2015; 33:4032–38. https://doi.org/10.1200/JCO.2015.63.2497.
6. Prahallad A, Sun C, Huang S, Di Nicolantonio F, Salazar R, Zecchin D, Beijersbergen RL, Bardelli A, Bernards R. Unresponsiveness of colon cancer to BRAF(V600E) inhibition through feedback activation of EGFR. Nature. 2012; 483:100–03. https://doi.org/10.1038/nature10868.
7. Popovici V, Budinska E, Tejpar S, Weinrich S, Estrella H, Hodgson G, Van Cutsem E, Xie T, Bosman FT, Roth AD, Delorenzi M. Identification of a poor-prognosis BRAF-mutant-like population of patients with colon cancer. J Clin Oncol. 2012; 30:1288–95. https://doi.org/10.1200/JCO.2011.39.5814.
8. Dalerba P, Sahoo D, Paik S, Guo X, Yothers G, Song N, Wilcox-Fogel N, Forgó E, Rajendran PS, Miranda SP, Hisamori S, Hutchison J, Kalisky T, et al. CDX2 as a Prognostic Biomarker in Stage II and Stage III Colon Cancer. N Engl J Med. 2016; 374:211–22. https://doi.org/10.1056/NEJMoa1506597.
9. Bae JM, Lee TH, Cho NY, Kim TY, Kang GH. Loss of CDX2 expression is associated with poor prognosis in colorectal cancer patients. World J Gastroenterol. 2015; 21:1457–67. https://doi.org/10.3748/wjg.v21.i5.1457.
10. Zlobec I, Bihl MP, Schwarb H, Terracciano L, Lugli A. Clinicopathological and protein characterization of BRAF- and K-RAS-mutated colorectal cancer and implications for prognosis. Int J Cancer. 2010; 127:367–80.
11. Jin-Song Y, Zhao-Xia W, Cheng-Yu L, Xiao-Di L, Ming S, Yuan-Yuan G, Wei D. Prognostic significance of Bcl-xL gene expression in human colorectal cancer. Acta Histochem. 2011; 113:810–14. https://doi.org/10.1016/j.acthis.2011.01.002.
12. Dukes CE, Bussey HJ. The spread of rectal cancer and its effect on prognosis. Br J Cancer. 1958; 12:309–20. https://doi.org/10.1038/bjc.1958.37.
13. Lindner AU, Salvucci M, Morgan C, Monsefi N, Resler AJ, Cremona M, Curry S, Toomey S, O'Byrne R, Bacon O, Stuhler M, Flanagan L, Wilson R, et al. BCL-2 system analysis identifies high-risk colorectal cancer patients. Gut. 2017; 66:2141–2148. https://doi.org/10.1136/gutjnl-2016-312287.
14. Certo M, Del Gaizo Moore V, Nishino M, Wei G, Korsmeyer S, Armstrong SA, Letai A. Mitochondria primed by death signals determine cellular addiction to antiapoptotic BCL-2 family members. Cancer Cell. 2006; 9:351–65. https://doi.org/10.1016/j.ccr.2006.03.027.
15. Sarosiek KA, Fraser C, Muthalagu N, Bhola PD, Chang W, McBrayer SK, Cantlon A, Fisch S, Golomb-Mello G, Ryan JA, Deng J, Jian B, Corbett C, et al. Developmental Regulation of Mitochondrial Apoptosis by c-Myc Governs Age- and Tissue-Specific Sensitivity to Cancer Therapeutics. Cancer Cell. 2017; 31:142–56. https://doi.org/10.1016/j.ccell.2016.11.011.
16. Faber AC, Coffee EM, Costa C, Dastur A, Ebi H, Hata AN, Yeo AT, Edelman EJ, Song Y, Tam AT, Boisvert JL, Milano RJ, Roper J, et al. mTOR inhibition specifically sensitizes colorectal cancers with KRAS or BRAF mutations to BCL-2/BCL-XL inhibition by suppressing MCL-1. Cancer

Discov. 2014; 4:42–52. https://doi.org/10.1158/2159-8290.CD-13-0315.

17. Lin L, Sabnis AJ, Chan E, Olivas V, Cade L, Pazarentzos E, Asthana S, Neel D, Yan JJ, Lu X, Pham L, Wang MM, Karachaliou N, et al. The Hippo effector YAP promotes resistance to RAF- and MEK-targeted cancer therapies. Nat Genet. 2015; 47:250–56. https://doi.org/10.1038/ng.3218.
18. Thorenoor N, Faltejskova-Vychytilova P, Hombach S, Mlcochova J, Kretz M, Svoboda M, Slaby O. Long non-coding RNA ZFAS1 interacts with CDK1 and is involved in p53-dependent cell cycle control and apoptosis in colorectal cancer. Oncotarget. 2016; 7:622–37. https://doi.org/10.18632/oncotarget.5807.
19. Bartkowiak K, Kwiatkowski M, Buck F, Gorges TM, Nilse L, Assmann V, Andreas A, Müller V, Wikman H, Riethdorf S, Schlüter H, Pantel K. Disseminated Tumor Cells Persist in the Bone Marrow of Breast Cancer Patients through Sustained Activation of the Unfolded Protein Response. Cancer Res. 2015; 75:5367–77. https://doi.org/10.1158/0008-5472.CAN-14-3728.
20. Bartkowiak K, Effenberger KE, Harder S, Andreas A, Buck F, Peter-Katalinic J, Pantel K, Brandt BH. Discovery of a novel unfolded protein response phenotype of cancer stem/progenitor cells from the bone marrow of breast cancer patients. J Proteome Res. 2010; 9:3158–68. https://doi.org/10.1021/pr100039d.
21. Tan K, Goldstein D, Crowe P, Yang JL. Uncovering a key to the process of metastasis in human cancers: a review of critical regulators of anoikis. J Cancer Res Clin Oncol. 2013; 139:1795–805. https://doi.org/10.1007/s00432-013-1482-5.
22. Guinney J, Dienstmann R, Wang X, de Reyniès A, Schlicker A, Soneson C, Marisa L, Roepman P, Nyamundanda G, Angelino P, Bot BM, Morris JS, Simon IM, et al. The consensus molecular subtypes of colorectal cancer. Nat Med. 2015; 21:1350–56. https://doi.org/10.1038/nm.3967.
23. Marisa L, de Reyniès A, Duval A, Selves J, Gaub MP, Vescovo L, Etienne-Grimaldi MC, Schiappa R, Guenot D, Ayadi M, Kirzin S, Chazal M, Fléjou JF, et al. Gene expression classification of colon cancer into molecular subtypes: characterization, validation, and prognostic value. PLoS Med. 2013; 10:e1001453. https://doi.org/10.1371/journal.pmed.1001453.
24. Bankhead P, Loughrey MB, Fernández JA, Dombrowski Y, McArt DG, Dunne PD, McQuaid S, Gray RT, Murray LJ, Coleman HG, James JA, Salto-Tellez M, Hamilton PW. QuPath: Open source software for digital pathology image analysis. Sci Rep. 2017; 7:16878. https://doi.org/10.1038/s41598-017-17204-5.

Bcl-xL as a poor prognostic biomarker and predictor of response to adjuvant chemotherapy specifically in *BRAF*-mutant stage II and III colon cancer

SUPPLEMENTARY MATERIALS

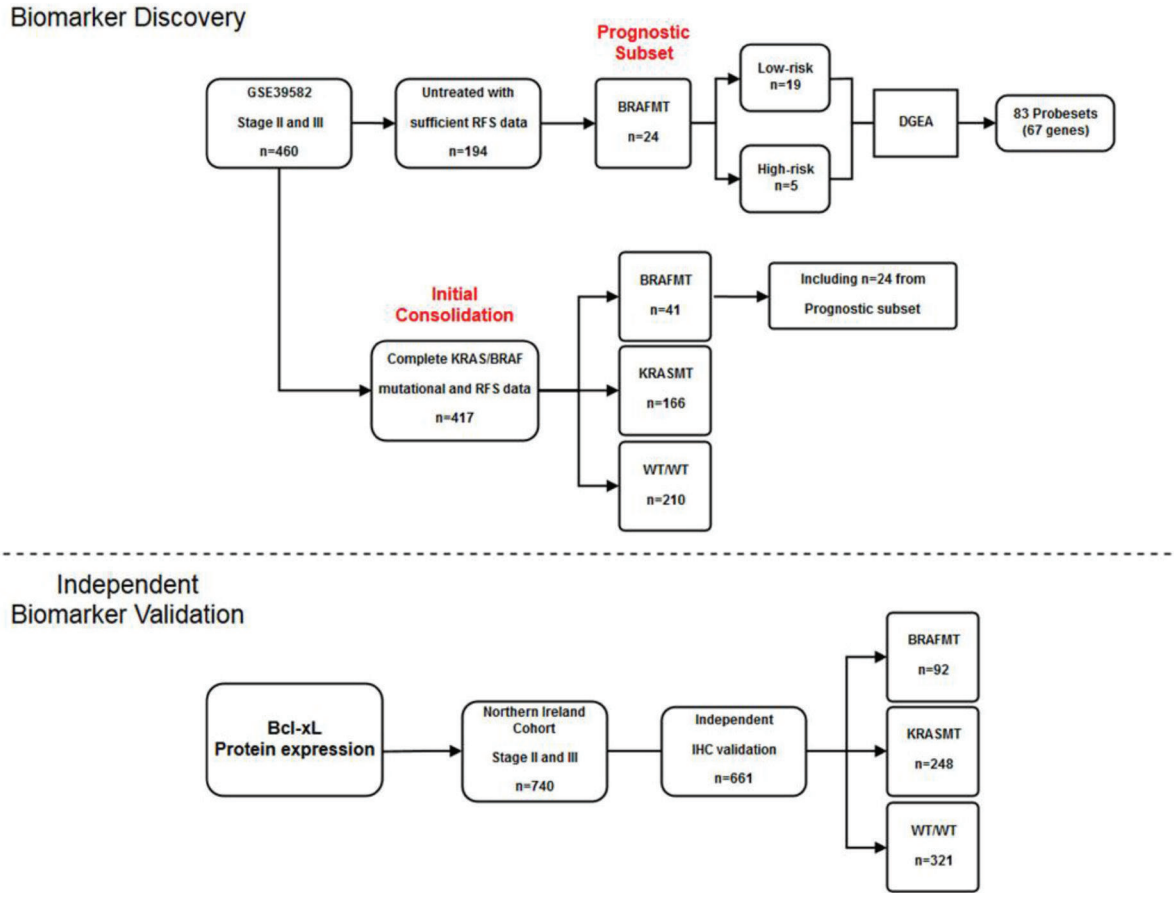

Supplementary Figure 1: Study overview of discovery and survival validation subsets. Biomarker Discovery: The data from GSE39582 was accessed through the NCBI GEO portal (https://www.ncbi.nlm.nih.gov/geo/). From the 566 Affymetrix U133 Plus 2.0 patient transcriptional profiles within this accession number, we selected profiles from stage II/III tumors with complete relapse data (n = 460 profiles). The "Prognostic Subset" was composed of *BRAFMT* and *KRASMT* tumors, which fulfilled risk filtering (see Methods) followed by differential gene expression analysis based on risk classification. *Bcl-xL* (and *ZFAS1*) were selected for relapse-free survival analyses using all stage II/III patients to create an "Initial Consolidation" subset (n = 417), which was composed of either *BRAFMT* (n = 41), *KRASMT* (n = 166) or *WT/WT* (n = 210) subgroups of samples. Independent Biomarker Validation: Patients from the Northern Ireland stage II/III cohort (n = 740) with clinical follow up and mutational status (n = 661) formed the "Independent IHC validation" cohort (described in detail in Methods) and contained *BRAFMT* (n = 92), *KRASMT* (n = 248) and *WT/WT* (n = 321) subgroups of patients.

A

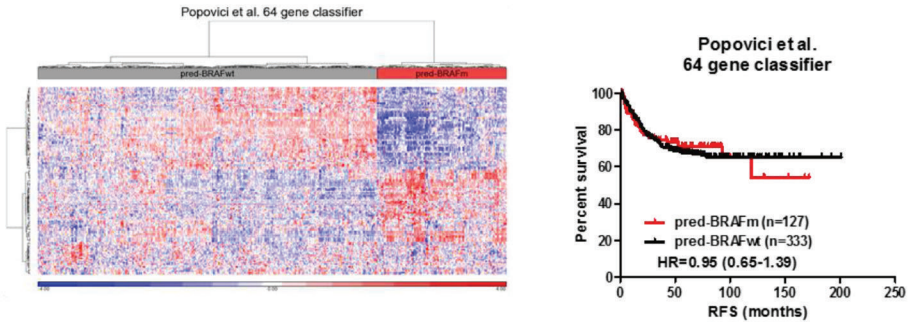

B

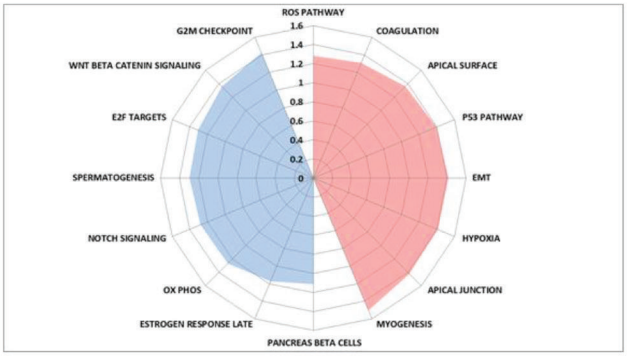

C

Cell Type	p-value(High vs. Low)	Ratio(High vs. Low)	Fold-Change(High vs. Low)	95% lower limit	95% upper limit
Fibroblasts	0.07	1.62	High up vs Low	-1.04	2.73
Cytotoxic lymphocytes	0.33	1.20	High up vs Low	-1.21	1.74
Monocytic lineage	0.36	1.20	High up vs Low	-1.24	1.79
Neutrophils	0.52	0.93	High down vs Low	-1.36	1.17
B lineage	0.54	0.85	High down vs Low	-2.06	1.48
NK cells	0.58	0.96	High down vs Low	-1.21	1.11
Endothelial cells	0.66	1.04	High up vs Low	-1.15	1.24
Myeloid dendritic cells	0.74	0.97	High down vs Low	-1.28	1.19
CD8 T cells	0.76	0.95	High down vs Low	-1.53	1.37
T cells	0.80	1.03	High up vs Low	-1.26	1.34

D

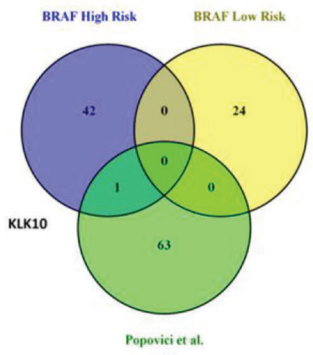

E

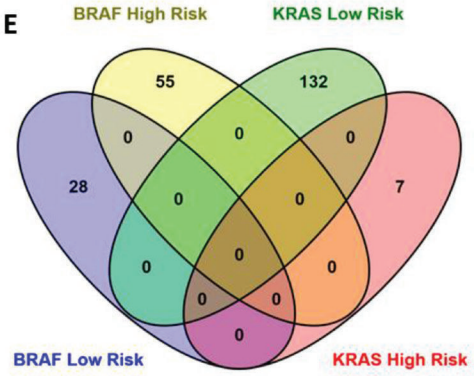

Supplementary Figure 2: Relapse risk analysis of previously published *BRAF* signature. (**A**) (Left) Hierarchical clustering using Ward and Euclidean metrics based on gene expression profiles of the 64 gene signature[4] (pred-BRAFm) using stage II/III CC transcription profiles from GSE39582 (n = 460) identified 2 distinct subgroups. (Right) Kaplan-Meier relapse survival analysis of these 2 subgroups (n = 333 vs n = 127) revealed no significant difference in relapse rates. Hazard Ratio (HR) and confidence interval calculated using log-rank method. (**B**) Radar plot depicting the enrichment scores from GSEA (http://software.broadinstitute.org/gsea/index.jsp) of high-risk and low-risk tumors used in the prognostic subset analysis. (**C**) Microenvironment Cell Populations-counter (MCP; https://doi.org/10.5281/zenodo.61372) analysis of high-risk and low-risk tumors used in the prognostic subset analysis. (**D**) Venn diagram analysis of our *BRAFMT* relapse risk genes compared to the previously published pred-BRAFm 64-gene signature from Popovici et al. [4] (**E**) Venn diagram comparative analysis of genes associated with risk of relapses in either *BRAFMT* or *KRASMT* genotypes revealed no overlap in the prognostic biology of these genotypes.

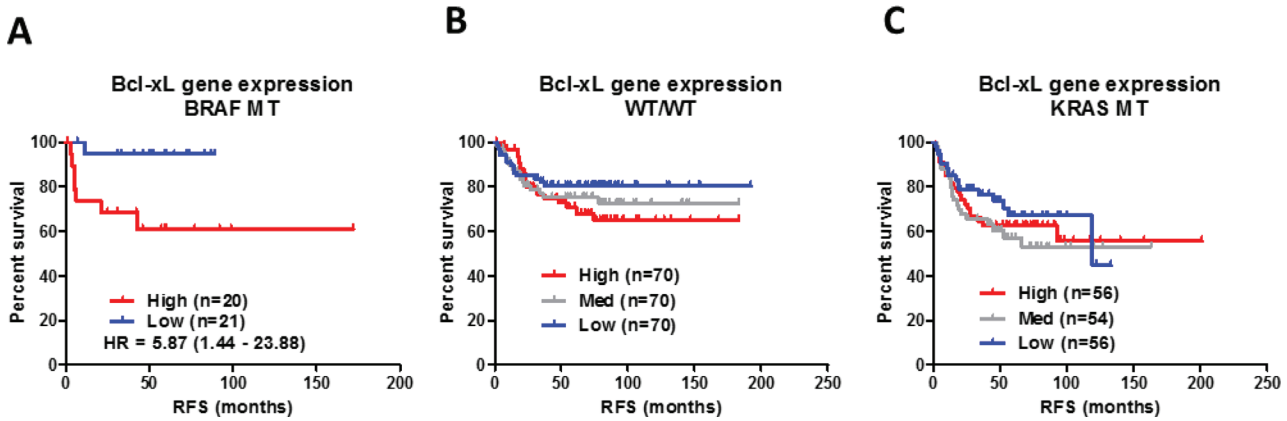

Supplementary Figure 3: Kaplan-Meier analyses of *Bcl-xL* relapse-free survival. (**A**) RFS analysis of *Bcl-xL* gene expression levels in *BRAFMT* tumors stratified on median gene expression. (**B**) RFS analysis of *Bcl-xL* gene expression levels in all *WT/WT* tumors. (**C**) RFS analysis of *Bcl-xL* gene expression levels in all *KRASMT* tumors. Unadjusted and adjusted HR statistics are detailed in Table 3.

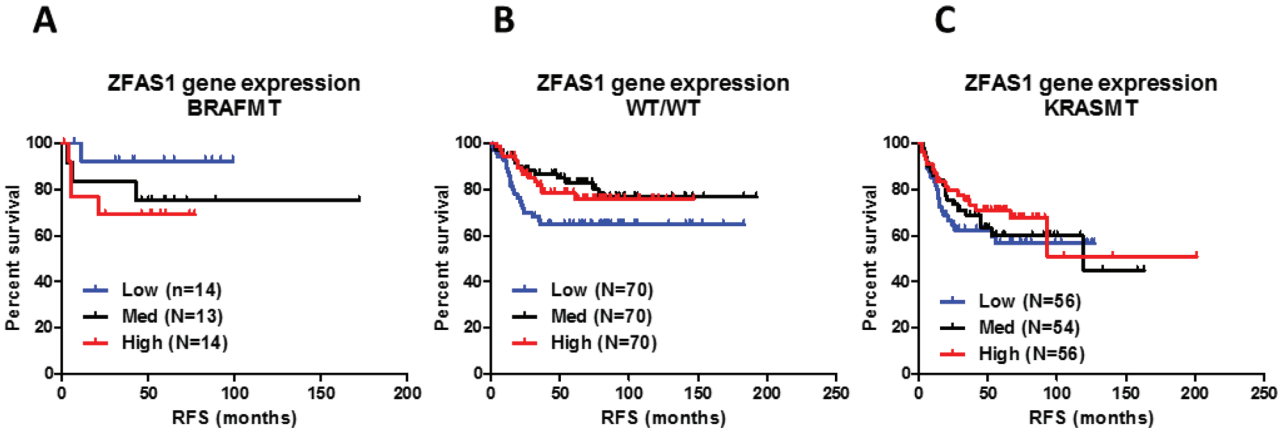

Supplementary Figure 4: Kaplan-Meier analyses of *ZFAS1* relapse-free survival. (**A–C**) RFS analysis of tertile stratified *ZFAS1* gene expression levels in *BRAFMT* (A), *WT/WT* (B) and *KRASMT* (C) stage II/III CRC patients (GSE39582). Unadjusted and adjusted HR statistics are detailed in Supplementary Table 3.

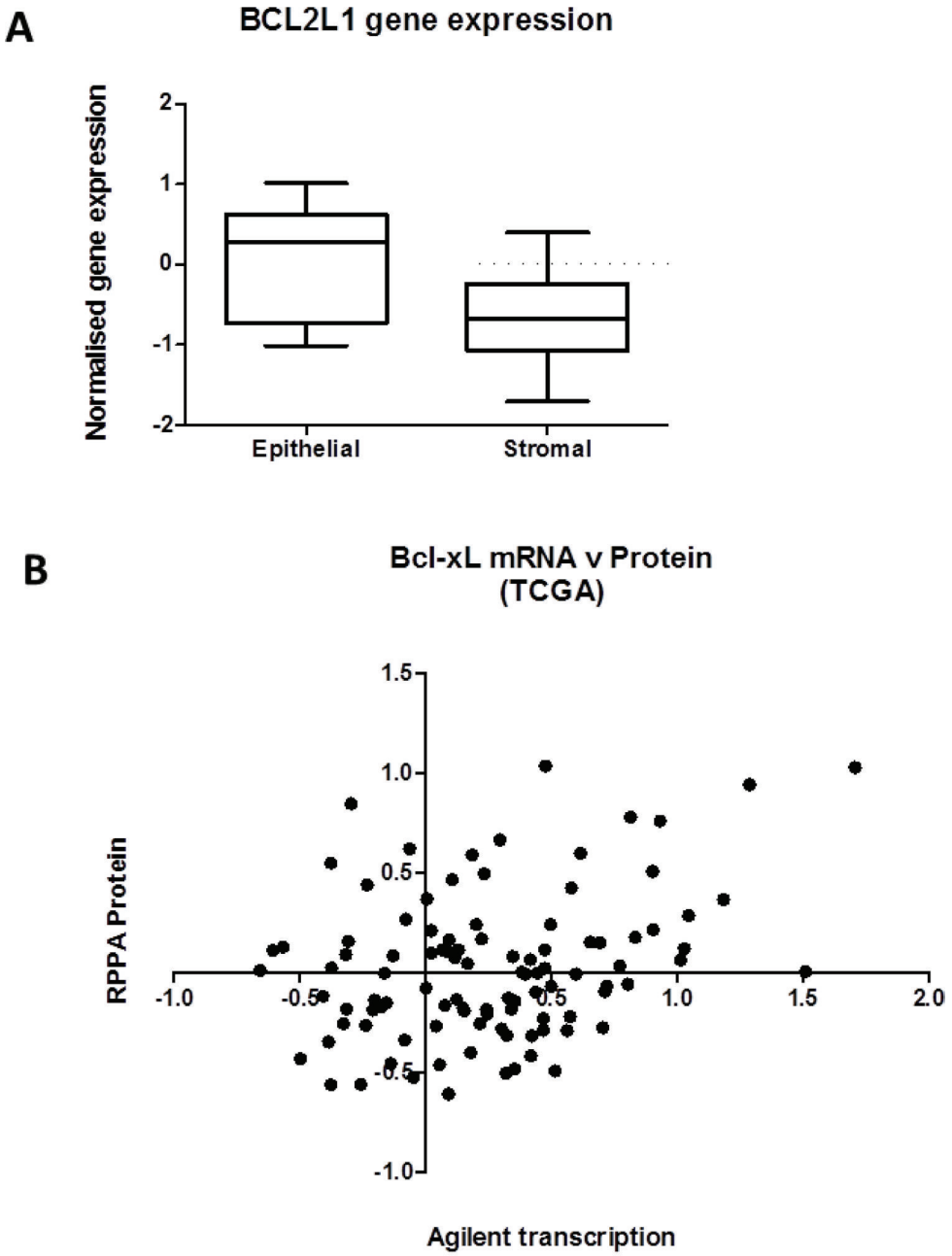

Number of XY Pairs	102
Pearson r	0.3129
95% confidence interval	0.1260 to 0.4783
P value (two-tailed)	0.0014
P value summary	**
Is the correlation significant? (alpha=0.05)	Yes

Supplementary Figure 5: *Bcl-xL* gene expression within the tumor microenvironment. (**A**) Analysis of *Bcl-xL* gene expression levels in stromal and epithelial components (GSE35602) highlights bimodal expression within the epithelial compartment. (**B**) Analysis of preprocessed mRNA (Agilent) and normalized protein (RPPA) data from the TCGA Firehose (https://gdac.broadinstitute.org/) indicated a significant correlation (Pearson's similarity) between *Bcl-xL* gene expression levels and protein expression.

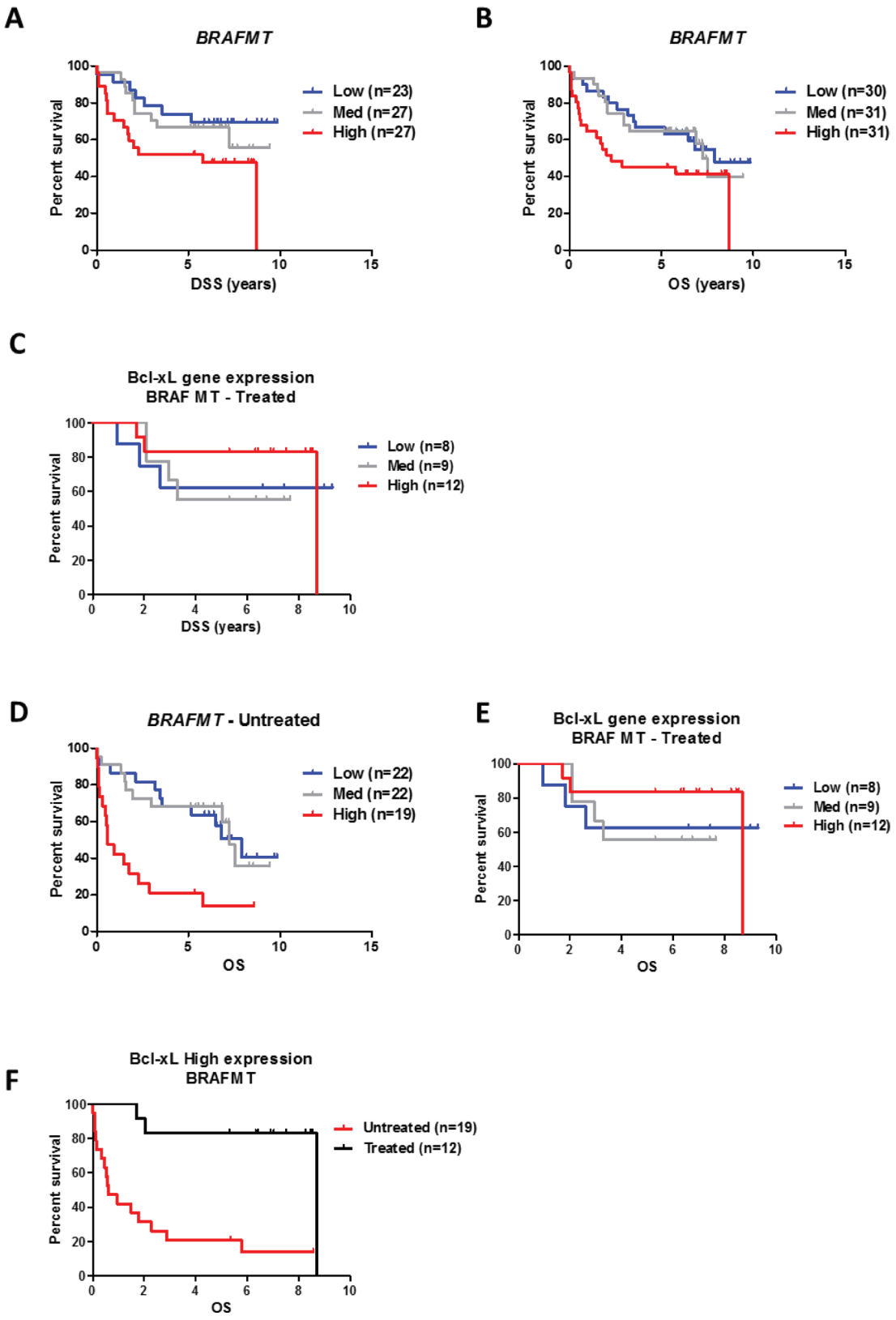

Supplementary Figure 6: Kaplan-Meier analyses of Bcl-xL overall- and disease-specific survival in independent validation cohort. (**A** and **B**) Overall survival (OS) and Disease-specific survival (DSS) curves using Kaplan-Meier estimation comparing tertile stratification of Bcl-xL protein expression (by IHC H-score) in all *BRAFMT* stage II/III CC patients. (**C**) DSS of Bcl-xL levels in treated *BRAFMT* tumors stratified by tertile. (**D** and **E**) Overall survival analysis of Bcl-xL protein expression levels in untreated and treated *BRAFMT* tumors stratified by tertile. Bcl-xL (**F**) Overall survival analysis of Bcl-xL-high protein expression in treated *BRAFMT* tumors. Unadjusted and adjusted HR statistics are detailed in Table 4.

Supplementary Table 1: Probesets significantly associated with relapse risk in *BRAFMT* tumors. See Supplementary_Table_1

Supplementary Table 2: Probesets significantly associated with relapse risk in *KRASMT* tumors. See Supplementary_Table_2

Supplementary Table 3: Unadjusted and adjusted analyses of relapse-free survival

ZFAS1	Non-progressors *n*	Progressors *n*	Unadjusted Hazard ratios (95% confidence intervals)	Adjusted** Hazard ratios (95% confidence intervals)
BRAF MT				
Low	13	1	1.00	1.00
Medium	10	3	3.50 (0.36–33.73)	3.09 (0.31–30.56)
High	10	4	4.69 (0.52–42.01)	4.71 (0.50–44.00)
KRAS MT				
Low	35	22	1.00	1.00
Medium	32	21	0.87 (0.47–1.62)	0.76 (0.41–1.42)
High	38	18	0.71 (0.37–1.33)	0.65 (0.34–1.24)
WT/WT				
Low	48	22	1.00	1.00
Medium	57	13	0.48 (0.24–0.95)	0.41 (0.20–0.82)
High	55	15	0.57 (0.30–1.10)	0.47 (0.24–0.92)

MT: Mutant; WT/WT: BRAF and KRAS wild-type.

*Cut-offs for low/medium/high NCRNA (ZFAS1) gene expression based on tertile values within each BRAF/KRAS status subgroup.

**Adjustments included age and sex, and were tested for TNM stage, MSI status, adjuvant chemotherapy receipt and tumour location for all models. A backwards elimination model was applied for tested confounders until all were significant at the $p < 0.25$ level in the model. Final adjustments included age, sex, and TNM stage (for BRAF MT); age, sex, TNM stage, adjuvant chemotherapy and tumour location (for KRAS MT); age, sex, TNM stage, MSI status and tumour location (for WT/WT).

RFS analysis was performed using Cox proportional hazards method in the *BRAFMT*, *KRASMT* or *WT/WT* stratified by *ZFAS1* expression levels. *Cut-offs for low/medium/high *ZFAS1* gene expression based on tertile values within each BRAF/KRAS status subgroup. **Adjustments included age and sex, and were tested for TNM stage, MSI status, adjuvant chemotherapy receipt and tumor location for all models. A backwards elimination model was applied for tested confounders until all were significant at the $p < 0.25$ level in the model. Final adjustments included age, sex, and TNM stage (for BRAF MT); age, sex, TNM stage, adjuvant chemotherapy and tumor location (for KRAS MT); age, sex, TNM stage, MSI status and tumor location (for WT/WT).

Supplementary Table 1: Probesets significantly associated with relapse risk in *BRAFMT* tumors

Column ID	Gene Symbol	p-value(Risk)	Fold-Change(High vs. Low)
201792_at	AEBP1	0.00357813	2.39615
204664_at	ALPP	0.0036019	1.88676
224339_s_at	ANGPTL1	0.000141463	1.92782
212312_at	BCL2L1	0.00253944	1.75675
206665_s_at	BCL2L1	0.00403036	1.841
215037_s_at	BCL2L1	0.00191145	1.9688
1569144_a_at	C9orf169	0.00268459	2.01757
208075_s_at	CCL7	0.000118381	2.22544
205627_at	CDA	0.000109302	7.0876
209383_at	DDIT3	0.000454073	1.81158
200666_s_at	DNAJB1	0.00158798	1.8228
200664_s_at	DNAJB1	0.00021294	2.00779
224825_at	DNTTIP1	0.000217611	2.0873
234942_s_at	DNTTIP1	6.34E-05	2.1421
203367_at	DUSP14	0.00352545	1.95014
206439_at	EPYC	0.00136055	3.66815
229521_at	FLJ36031	0.00446205	1.87711
226847_at	FST	0.00409711	1.82151
224252_s_at	FXYD5	0.00452331	1.95374
204457_s_at	GAS1	0.00206559	4.65337
215243_s_at	GJB3	0.00398615	2.60134
206156_at	GJB5	0.00102843	2.39729
45714_at	HCFC1R1	0.00279056	1.82102
117_at	HSPA6	0.000228093	2.59902
213418_at	HSPA6	0.000539337	3.51734
226559_at	IER5L	0.00289594	1.86633
203851_at	IGFBP6	0.0049927	3.44117
215808_at	KLK10	0.00157391	2.12964
209800_at	KRT16	0.00132379	2.30971
214580_x_at	KRT6A /// KRT6B /// KRT6C	0.00213891	2.01611
244740_at	LOC100128252	0.000395352	1.78227
225381_at	LOC399959	0.00321655	5.10276
210605_s_at	MFGE8	0.00168213	1.93601
208148_at	MYH4	0.00187218	1.88317
226227_x_at	NCRNA00275	0.00102301	1.82659
224915_x_at	NCRNA00275	0.000814649	1.85619
226835_s_at	NCRNA00275	0.00101009	1.89756
225930_at	NKIRAS1	0.00158521	1.75339
220106_at	NPC1L1	0.00210857	1.9331
227486_at	NT5E	0.000965098	2.69796
206859_s_at	PAEP	0.00310726	3.14511
218273_s_at	PDP1	0.00474931	2.04182

222572_at	PDP1	0.00161747	2.24056
218634_at	PHLDA3	0.00337563	2.13164
202014_at	PPP1R15A	0.00414088	1.7996
37028_at	PPP1R15A	0.00489879	1.81077
237732_at	PRR9	0.00117195	1.8945
205228_at	RBMS2	0.001113	1.76487
204337_at	RGS4	0.00161388	3.08886
204743_at	TAGLN3	0.00295239	1.80623
228121_at	TGFB2	0.00279341	1.91989
207426_s_at	TNFSF4	0.00335822	2.3434
203683_s_at	VEGFB	0.001539	1.77802

Column ID	**Gene Symbol**	**p-value(Risk)**	**Fold-Change(High vs. Low)**
209173_at	AGR2	0.00263761	-2.7237
213143_at	C2orf72	0.00232002	-1.98416
242447_at	C3orf70	0.000112081	-3.83449
235562_at	C3orf70	0.00349908	-1.95876
213050_at	COBL	0.00351991	-1.82387
214106_s_at	GMDS	0.0045034	-2.53458
226446_at	HES6	0.00336194	-2.35981
203126_at	IMPA2	0.00231815	-1.95056
226248_s_at	KIAA1324	0.0021877	-6.44242
225525_at	KIAA1671	0.00233745	-1.78939
227250_at	KREMEN1	0.00109032	-1.75114
215543_s_at	LARGE	0.000940792	-1.97306
236118_at	LOC100128893	0.00240066	-2.3928
238956_at	LOC100506781	0.000595672	-3.19352
206418_at	NOX1	0.0036011	-5.46402
207217_s_at	NOX1	0.00473879	-3.70583
226499_at	NRARP	0.00325207	-2.25952
205251_at	PER2	0.00356648	-2.22784
205632_s_at	PIP5K1B	0.0020144	-4.12775
242055_at	PSMG4	0.00289168	-2.4234
203625_x_at	SKP2	0.0043362	-1.75644
223194_s_at	SLC22A23	0.00277791	-2.35077
212458_at	SPRED2	0.00151256	-1.86388
213285_at	TMEM30B	0.0019072	-2.48282
36742_at	TRIM15	0.00348685	-1.95849
217979_at	TSPAN13	0.0010721	-2.12954

Supplementary Table 2: Probesets significantly associated with relapse risk in *KRASMT* tumors.

Column ID	Gene Symbol	p-value(Risk)	Fold-Change(High vs. Low)
206208_at	CA4	0.00389026	1.81044
206209_s_at	CA4	0.00461504	2.39118
231814_at	MUC12	0.00247551	2.5351
231941_s_at	MUC20	0.00435644	1.91621
201481_s_at	PYGB	0.00213036	1.85362
205464_at	SCNN1B	0.000441448	1.84519
218345_at	TMEM176A	0.000936925	1.85153

Column ID	Gene Symbol	p-value(Risk)	Fold-Change(High vs. Low)
228241_at	AGR3	0.00346503	-2.75387
222108_at	AMIGO2	0.00322124	-1.87098
201012_at	ANXA1	0.000205205	-2.05865
204205_at	APOBEC3G	8.38E-05	-1.85521
235333_at	B4GALT6	1.30E-05	-1.75234
209406_at	BAG2	0.00183076	-2.08003
203685_at	BCL2	4.53E-05	-1.79155
205681_at	BCL2A1	0.000757676	-2.15802
210538_s_at	BIRC3	9.95E-06	-2.12007
221478_at	BNIP3L	2.30E-05	-1.95538
238794_at	C10orf78	0.000127179	-1.83311
1552701_a_at	CARD16	0.000128506	-1.79847
1552703_s_at	CARD16 /// CASP1	0.000614458	-1.83203
211368_s_at	CASP1	0.00146134	-1.94838
206011_at	CASP1	0.00333069	-1.93386
52285_f_at	CEP76	1.19E-06	-2.11923
219311_at	CEP76	8.38E-07	-1.83853
1555564_a_at	CFI	0.000432979	-2.36342
203854_at	CFI	0.000791105	-2.06731
235117_at	CHAC2	6.64E-06	-2.01533
209732_at	CLEC2B	0.000106237	-1.82715
205159_at	CSF2RB	0.000709512	-1.76088
204533_at	CXCL10	0.000180474	-2.52959
211122_s_at	CXCL11	0.00127775	-3.03047
210163_at	CXCL11	0.000889939	-2.72659
205242_at	CXCL13	0.00140635	-2.44987
203915_at	CXCL9	0.000268626	-2.56936
209606_at	CYTIP	0.00113889	-1.75922
202843_at	DNAJB9	5.84E-07	-1.89348
225502_at	DOCK8	0.0011122	-1.77308
218854_at	DSE	0.00134482	-1.75697
221773_at	ELK3	6.71E-07	-1.77531
222646_s_at	ERO1L	0.000176027	-1.85066

218498_s_at	ERO1L	3.07E-05	-1.84758
229390_at	FAM26F	0.00409905	-1.75745
225734_at	FBXO22	8.05E-07	-1.75456
204007_at	FCGR3B	0.00338066	-1.7828
233898_s_at	FGFR1OP2	5.58E-07	-1.80289
227265_at	FGL2	6.42E-05	-1.93117
203988_s_at	FUT8	2.56E-06	-2.00595
205890_s_at	GABBR1 /// UBD	0.000433147	-2.38637
201724_s_at	GALNT1	4.81E-06	-1.8049
238756_at	GAS2L3	0.000100668	-1.81197
202270_at	GBP1	0.000188763	-2.01793
231577_s_at	GBP1	0.00105324	-1.77853
232024_at	GIMAP2	0.000872061	-1.77736
205488_at	GZMA	0.00014183	-2.0867
225297_at	HAUS1	7.38E-08	-1.82549
228697_at	HINT3	0.00412929	-1.92596
202557_at	HSPA13	8.02E-05	-1.81863
208965_s_at	IFI16	0.000777373	-1.77098
206332_s_at	IFI16	9.67E-05	-1.75571
214453_s_at	IFI44	0.00364683	-1.78752
204415_at	IFI6	0.00385941	-1.98368
229450_at	IFIT3	0.00121184	-1.96725
206693_at	IL7	0.000185792	-1.81806
202859_x_at	IL8	0.000801206	-2.31049
222698_s_at	IMPACT	9.21E-09	-2.1685
218637_at	IMPACT	1.58E-07	-1.9318
217894_at	KCTD3	1.07E-06	-1.80463
229850_at	KDSR	1.38E-06	-1.93273
1558279_a_at	KDSR	1.08E-05	-1.79319
226534_at	KITLG	7.40E-06	-1.8462
217388_s_at	KYNU	5.64E-05	-2.26288
218701_at	LACTB2	0.00010935	-1.75318
213880_at	LGR5	0.00356176	-2.67238
241607_at	LOC730102	0.00428868	-1.76394
206584_at	LY96	5.88E-05	-2.11143
1555745_a_at	LYZ	0.000477335	-4.07836
213975_s_at	LYZ	0.000721143	-1.89033
225160_x_at	MDM2	6.02E-06	-1.89405
229711_s_at	MDM2	1.26E-05	-1.78364
224725_at	MIB1	5.83E-05	-1.86032
224720_at	MIB1	3.87E-05	-1.75778
204580_at	MMP12	0.000284165	-2.26718
204162_at	NDC80	8.86E-06	-1.85885
226810_at	OGFRL1	5.97E-05	-1.85241
219148_at	PBK	0.00104853	-1.95683
226452_at	PDK1	0.000114157	-1.77671

225688_s_at	PHLDB2	0.00217506	-1.85285
210145_at	PLA2G4A	0.00144242	-2.58431
213241_at	PLXNC1	0.00108721	-1.80079
204286_s_at	PMAIP1	2.41E-05	-1.96477
204285_s_at	PMAIP1	0.000110465	-1.93898
209598_at	PNMA2	0.000278485	-2.43892
204748_at	PTGS2	0.00120791	-2.2952
212588_at	PTPRC	0.000175817	-1.96745
228708_at	RAB27B	7.33E-05	-2.64312
213982_s_at	RABGAP1L	1.04E-08	-1.76329
204070_at	RARRES3	0.00289131	-1.83599
205590_at	RASGRP1	2.54E-05	-1.76193
203344_s_at	RBBP8	1.60E-06	-1.77849
225202_at	RHOBTB3	0.000567503	-1.93838
235199_at	RNF125	0.00245966	-1.80438
239143_x_at	RNF138	1.30E-07	-1.77486
225541_at	RPL22L1	5.69E-07	-2.48396
225953_at	RPRD1A	1.45E-06	-1.75702
213262_at	SACS	0.000159156	-1.85171
228653_at	SAMD5	0.00146913	-2.43295
242626_at	SAMD5	0.00137079	-2.30313
226603_at	SAMD9L	0.00145733	-1.78907
220330_s_at	SAMSN1	4.77E-05	-1.99031
205352_at	SERPINI1	0.000172412	-1.79134
212989_at	SGMS1	2.32E-05	-1.75506
222838_at	SLAMF7	0.000516181	-1.93411
232277_at	SLC28A3	0.000367502	-2.24888
202088_at	SLC39A6	2.90E-08	-1.75224
202527_s_at	SMAD4	1.33E-05	-1.85357
212569_at	SMCHD1	5.28E-06	-1.79771
227542_at	SOCS6	6.08E-06	-1.82359
1566342_at	SOD2	6.32E-05	-1.77182
202817_s_at	SS18	3.66E-06	-2.01561
217790_s_at	SSR3	0.00013578	-1.79882
205542_at	STEAP1	0.00100237	-1.76219
230560_at	STXBP6	0.00210149	-1.78162
208986_at	TCF12	6.64E-06	-1.80339
205943_at	TDO2	0.00376235	-2.00209
224793_s_at	TGFBR1	1.76E-05	-1.82457
226117_at	TIFA	5.47E-08	-1.79069
219410_at	TMEM45A	0.00146413	-2.01775
206026_s_at	TNFAIP6	0.00291042	-2.10577
210260_s_at	TNFAIP8	1.78E-06	-2.01469
208296_x_at	TNFAIP8	1.48E-06	-1.9402
210643_at	TNFSF11	0.00127014	-1.86161
223502_s_at	TNFSF13B	4.51E-05	-2.09115

223501_at	TNFSF13B	4.54E-05	-2.0025
213293_s_at	TRIM22	0.00230209	-1.75456
225406_at	TWSG1	1.74E-05	-1.83641
222731_at	ZDHHC2	0.000532781	-2.1027